Electronic Supplementary Information for

Photoinduced hydrogen-bonded self-assembly of cation-capped complexes and novel photoswitchable supramolecular devices based on (aza)-18-crown-6-containing styryl dyes bearing a long *N*-ammonioalkyl substituent

Sergey P. Gromov,[a,b,]* Timofey P. Martyanov,[a,c] Artem I. Vedernikov,[a] Svetlana N. Dmitrieva,[a] Dmitry V. Kondratuk,[a] Artem P. Vorozhtsov,[a,c] and Evgeny N. Ushakov[a,c,]*

[a] Photochemistry Center of RAS, FSRC "Crystallography and Photonics", Russian Academy of Sciences, Novatorov str. 7A-1, Moscow 119421, Russian Federation
E-mail addresses: spgromov@mail.ru (S.P. Gromov), artem_vedernikov@mail.ru (A.I. Vedernikov), sveta-dsn@bk.ru (S.N. Dmitrieva), dmitry.kondratiuk@gmail.com (D.V. Kondratuk)
[b] Department of Chemistry, Lomonosov Moscow State University, Leninskie Gory 1-3, Moscow 119991, Russian Federation
[c] Federal Research Center of Problems of Chemical Physics and Medicinal Chemistry, Russian Academy of Sciences, Chernogolovka, Moscow Region 142432, Russian Federation
E-mail address: martyanov.t@gmail.ru (T.P. Martyanov), artem2001qaz@gmail.com (A.P. Vorozhtsov), e.n.ushakov@gmail.com (E.N. Ushakov)

* Corresponding authors.

Table of Contents

I   General methods and synthetic procedures

The ^{1}H and ^{13}C NMR spectra were recorded on a Bruker DRX500 instrument in DMSO-d_6 and MeCN-d_3 using the solvent as the internal standard (δ_H 2.50 and 1.96, respectively, and δ_C 39.43 for DMSO-d_6). Chemical shifts were measured to an accuracy of 0.01 ppm, and spin-spin coupling constants were determined to an accuracy of 0.1 Hz. The samples for elemental analysis were dried at 80 °C *in vacuo*. Electronic absorption spectra were recorded on a Specord M40 spectrophotometer in quartz cells with ground-in stoppers. MeCN (special purity grade, water content < 0.03%, v/v, Cryochrom) was used to prepare solutions. Ca(ClO$_4$)$_2$ and Ba(ClO$_4$)$_2$ were dried *in vacuo* at 230 °C, and NaClO$_4$ was dried *in vacuo* at 170 °C. Tetrabutylammonium perchlorate (Bu$_4$NClO$_4$, Sigma-Aldrich, for electrochemical analysis, ≥99%) was used without additional purification.

Synthetic procedures. 4'-Formylbenzo-18-crown-6 ether,[1] *N*-methyl(5'-formylbenzo)aza-18-crown-6 ether,[2] 5-bromopentylammonium bromide,[3] 4-(bromomethyl)benzylammonium bromide,[4] and styryl dyes (*E*)-**1d**,[5] (*E*)-**1e**,[6] and (*E*)-**2b**[7] were synthesized as described in literature.

3-(6-Ammoniohexyl)-2-methyl-1,3-benzothiazol-3-ium diperchlorate (**3a**) was prepared by a known procedure[6]; ^{13}C NMR (125.76 MHz, 24 °C) δ 16.75 (Me), 25.20 and 25.26 (*C*H$_2$CH$_2$CH$_2$CH$_2$N), 26.66 (*C*H$_2$CH$_2$NH$_3$), 27.50 (*C*H$_2$CH$_2$N), 38.62 (*C*H$_2$NH$_3$), 48.98 (*C*H$_2$N), 116.75 (4-C), 124.57 (7-C), 128.04 (6-C), 129.05 (7a-C), 129.29 (5-C), 140.74 (3a-C), 177.05 (2-C) ppm.

3-[4-(Ammoniomethyl)benzyl]-2-methyl-1,3-benzothiazol-3-ium diperchlorate (**3b**). A mixture of 4-(bromomethyl)benzylammonium bromide (0.1 g, 0.36 mmol) and 2-methylbenzothiazole (0.4 mL, 3.15 mmol) was heated at 100 °C (oil bath) for 12 h. After cooling to room temperature, the reaction mixture was washed with trituration with benzene (3 × 3 mL), then with acetone (3 × 3 mL) and then with chloroform (3 × 3 mL). The insoluble residue (67 mg) was dissolved in a minimum quantity of hot MeOH; and HClO$_4$ (70%, aq.) (40 μL, 0.46 mmol) was added. After cooling to room temperature, Et$_2$O (10 mL) was added to the mixture, and the crystalline precipitate thus formed was collected on a filter, washed with Et$_2$O (2 × 5 mL), and dried in air to give compound **3b** (39 mg, 23% yield) as yellowish crystals, mp 205–208 °C; ^{1}H NMR (500.13 MHz, DMSO-d_6, 30 °C) δ 3.26 (s, 3H, Me), 4.02 (m, 2H, C*H$_2$*NH$_3$), 6.09 (s, 2H, CH$_2$N), 7.37 (d, ^3J = 8.4 Hz, 2H, 3'-H, 5'-H), 7.45 (d, ^3J = 8.4 Hz, 2H, 2'-H, 6'-H), 7.81 (m, 2H, 5-H, 6-H), 8.06 (br s, 3H, NH$_3$), 8.12 (d, ^3J = 8.4 Hz, 1H, 4-H), 8.48 (d, ^3J = 8.4 Hz, 1H, 7-H) ppm; ^{13}C NMR (125.76 MHz, 24 °C) δ 17.15 (Me), 41.73 (*C*H$_2$NH$_3$), 51.52 (*C*H$_2$N), 116.91 (4-C), 124.77 (7-C), 127.21 (2'-C, 6'-C), 128.21 (6-C), 129.22 (7a-C), 129.41 (5-C),

129.49 (3'-C, 5'-C), 133.00 (4'-C), 134.25 (1'-C), 140.74 (3a-C), 178.52 (2-C) ppm. Anal. calcd for $C_{16}H_{18}Cl_2N_2O_8S$ (469.29): C, 40.95; H, 3.87; N, 5.97. Found: C, 41.06; H, 4.00; N, 6.10%.

3-(5-Ammoniopentyl)-2-methyl-1,3-benzothiazol-3-ium diperchlorate (**3c**). A mixture of 5-bromopentylammonium bromide (0.50 g, 2 mmol) and 2-methylbenzothiazole (0.51 mL, 4 mmol) was heated at 160 °C (oil bath) for 18 h. After cooling to room temperature, the reaction mixture was washed with trituration with benzene (2 × 3 mL), then with acetone (2 × 3 mL), and then with chloroform (3 × 3 mL). The insoluble residue (0.30 g) was dissolved in a minimum quantity of hot MeOH; and $HClO_4$ (70%, aq.) (0.16 mL, 1.83 mmol) was added. After cooling to room temperature, Et_2O (20 mL) was added to the mixture, and the precipitate thus formed was collected on a filter, washed with Et_2O (2 × 5 mL), and dried in air to give compound **3c** (0.30 g, 34% yield) as a light brownish powder, mp 170–172 °C; ^{1}H NMR (500.13 MHz, DMSO-d_6, 30 °C) δ 1.45 (m, 2H, CH_2CH$_2$CH$_2$N), 1.56 (m, 2H, CH_2CH$_2$NH$_3$), 1.86 (m, 2H, CH_2CH$_2$N), 2.78 (m, 2H, CH_2NH$_3$), 3.21 (s, 3H, Me), 4.69 (t, ^3J = 7.7 Hz, 2H, CH$_2$N), 7.59 (br s, 3H, NH$_3$), 7.81 (m, 1H, 6-H), 7.90 (m, 1H, 5-H), 8.33 (d, ^3J = 8.6 Hz, 1H, 4-H), 8.45 (d, ^3J = 8.2 Hz, 1H, 7-H) ppm; ^{13}C NMR (125.76 MHz, 24 °C) δ 16.73 (Me), 22.65 (CH$_2$CH$_2$CH$_2$N), 26.52 (CH$_2$CH$_2$NH$_3$), 27.13 (CH$_2$CH$_2$N), 38.48 (CH$_2$NH$_3$), 48.94 (CH$_2$N), 116.77 (4-C), 124.56 (7-C), 128.07 (6-C), 129.03 (7a-C), 129.31 (5-C), 140.76 (3a-C), 177.16 (2-C) ppm. Anal. calcd for $C_{13}H_{20}Cl_2N_2O_8S$ (435.28): C, 35.87; H, 4.63; N, 6.44. Found: C, 35.80; H, 4.72; N, 6.28%.

3-(6-Ammoniohexyl)-2-[(E)-2-(2,3,5,6,8,9,11,12,14,15-decahydro-1,4,7,10,13,16-benzohexaoxacyclooctadecin-18-yl)vinyl]-1,3-benzothiazol-3-ium diperchlorate [(*E*)-**1a**] was prepared by a known procedure[6]; ^{13}C NMR (125.76 MHz, 30 °C) δ 25.11 and 25.26 (CH$_2$CH$_2$CH$_2$CH$_2$N), 26.66 (CH$_2$CH$_2$NH$_3$), 28.41 (CH$_2$CH$_2$N), 38.67 (CH$_2$NH$_3$), 48.45 (CH$_2$N), 68.30 (CH$_2$OAr), 68.34 and 68.43 (CH$_2$OAr, CH$_2$CH$_2$OAr), 68.50 (CH$_2$CH$_2$OAr), 69.55 (CH$_2$O), 69.64 (CH$_2$O), 69.68 (2 CH$_2$O), 69.80 (CH$_2$O), 69.83 (CH$_2$O), 110.63 (HC=CHHet), 112.64 (20-C), 113.01 (17-C), 116.51 (4-C), 124.21 (7-C), 125.59 (19-C), 126.78 (18-C), 127.84 (7a-C), 128.16 (6-C), 129.30 (5-C), 141.12 (3a-C), 148.31 (16a-C), 149.47 (HC=CHHet), 152.42 (20a-C), 171.87 (2-C) ppm.
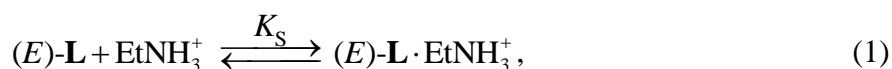
3-[4-(Ammoniomethyl)benzyl]-2-[(E)-2-(2,3,5,6,8,9,11,12,14,15-decahydro-1,4,7,10,13,16-benzohexaoxacyclooctadecin-18-yl)vinyl]-1,3-benzothiazol-3-ium diperchlorate [(*E*)-**1b**]. A mixture of compound **3b** (27 mg, 58 µmol), 4'-formylbenzo-18-crown-6 ether (22 mg, 65 µmol), and abs. EtOH (3 mL) was heated at 80 °C for 125 h. After cooling to room temperature, the precipitate thus formed was collected on a filter, washed with cold CH_2Cl_2 (0.5 mL), and then dissolved in MeCN (30 mL). The solution was filtered and then evaporated *in vacuo* to give dye (*E*)-**1b** (23 mg, 50% yield) as a yellow-orange fine-grained solid, mp 207–208 °C; ^{1}H NMR
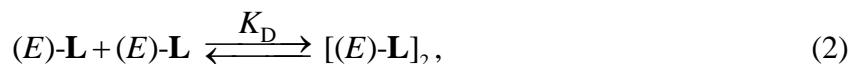
(500.13 MHz, DMSO-d_6, 24 °C) δ 3.53 (s, 4H, 2 CH$_2$O), 3.57 (m, 4H, 2 CH$_2$O), 3.63 (m, 4H, 2 CH$_2$O), 3.79 (m, 2H, CH_2CH$_2$OAr), 3.82 (m, 2H, CH_2CH$_2$OAr), 3.99 (m, 2H, CH_2NH$_3$), 4.21 (m, 4H, 2 CH_2OAr), 6.28 (s, 2H, CH$_2$N), 7.16 (d, ^3J = 8.6 Hz, 1H, 20-H), 7.41 (d, ^3J = 8.4 Hz, 2H, 3'-H, 5'-H), 7.44 (d, ^3J = 8.4 Hz, 2H, 2'-H, 6'-H), 7.62 (br d, ^3J = 8.6 Hz, 1H, 19-H), 7.65 (br s, 1H, 17-H), 7.76 (m, 1H, 6-H), 7.80 (m, 1H, 5-H), 8.00 (d, ^3J = 15.7 Hz, 1H, HC=CHHet), 8.05 (br m, 3H, NH$_3$), 8.11 (d, ^3J = 8.2 Hz, 1H, 4-H), 8.26 (d, ^3J = 15.7 Hz, 1H, HC=CHHet), 8.45 (d, ^3J = 7.7 Hz, 1H, 7-H) ppm; ^{13}C NMR (125.76 MHz, 25 °C) δ 41.74 (CH$_2$NH$_3$), 50.89 (CH$_2$N), 68.34 and 68.37 (2 CH$_2$OAr, CH$_2$CH$_2$OAr), 68.45 (CH$_2$$CH_2$OAr), 69.58 (CH$_2$O), 69.67 (CH$_2$O), 69.71 (2 CH$_2$O), 69.83 (CH$_2$O), 69.86 (CH$_2$O), 110.58 (HC=$C$HHet), 112.48 (20-C), 112.62 (17-C), 116.67 (4-C), 124.45 (7-C), 126.16 (19-C), 126.76 (18-C), 127.17 (2'-C, 6'-C), 127.90 (7a-C), 128.27 (6-C), 129.40 (5-C), 129.54 (3'-C, 5'-C), 134.17 and 134.20 (1'-C, 4'-C), 141.07 (3a-C), 148.42 (16a-C), 150.46 (HC=CHHet), 152.72 (20a-C), 173.04 (2-C) ppm; UV–vis (MeCN) λ_{max} (ε) = 425 nm (29400 M^{-1} cm^{-1}). Anal. calcd for C$_{33}$H$_{40}$Cl$_2$N$_2$O$_{14}$S (791.65): C, 50.07; H, 5.09; N, 3.54. Found: C, 50.05; H, 5.21; N, 3.53%.

3-(5-Ammoniopentyl)-2-[(E)-2-(2,3,5,6,8,9,11,12,14,15-decahydro-1,4,7,10,13,16-benzohexaoxacyclooctadecin-18-yl)vinyl]-1,3-benzothiazol-3-ium diperchlorate [(*E*)-**1c**]. A mixture of compound **3c** (70 mg, 0.16 mmol), 4'-formylbenzo-18-crown-6 ether (60 mg, 0.18 mmol), and abs. EtOH (5 mL) was heated at 80 °C for 125 h. After cooling to room temperature, the precipitate formed was collected on a filter, washed with abs. EtOH (2 mL) and then with benzene (3 mL), and dried in air to give dye (*E*)-**1c** (76 mg, 60% yield) as a yellow-orange powder, mp 185–186 °C; ^{1}H NMR (500.13 MHz, DMSO-d_6, 30 °C) δ 1.44 (m, 2H, CH_2CH$_2$CH$_2$N), 1.55 (m, 2H, CH_2CH$_2$NH$_3$), 1.86 (m, 2H, CH_2CH$_2$N), 2.74 (m, 2H, CH_2NH$_3$), 3.54 (s, 4H, 2 CH$_2$O), 3.57 (m, 4H, 2 CH$_2$O), 3.64 (m, 4H, 2 CH$_2$O), 3.80 (m, 2H, CH_2CH$_2$OAr), 3.83 (m, 2H, CH_2CH$_2$OAr), 4.23 (m, 4H, 2 CH_2OAr), 4.93 (t, ^3J = 6.8 Hz, 2H, CH$_2$N), 7.17 (d, ^3J = 8.2 Hz, 1H, 20-H), 7.55 (br s, 3H, NH$_3$), 7.66 (br s, 1H, 17-H), 7.67 (br d, ^3J = 8.2 Hz, 1H, 19-H), 7.79 (m, 1H, 6-H), 7.84 (d, ^3J = 15.7 Hz, 1H, HC=CHHet), 7.87 (m, 1H, 5-H), 8.19 (d, ^3J = 15.7 Hz, 1H, HC=CHHet), 8.25 (d, ^3J = 8.6 Hz, 1H, 4-H), 8.43 (d, ^3J = 8.2 Hz, 1H, 7-H) ppm; ^{13}C NMR (125.76 MHz, 30 °C) δ 22.53 (CH$_2$$CH_2CH_2$N), 26.60 (CH$_2$$CH_2NH_3$), 28.06 ($CH_2CH_2$N), 38.45 (CH$_2NH_3$), 48.42 (CH$_2$N), 68.36 and 68.45 (2 CH$_2$OAr, CH$_2$CH$_2$OAr), 68.51 (CH$_2$$CH_2$OAr), 69.58 (CH$_2$O), 69.69 (3 CH$_2$O), 69.82 (CH$_2$O), 69.85 (CH$_2$O), 110.66 (HC=$C$HHet), 112.69 (20-C), 113.16 (17-C), 116.55 (4-C), 124.21 (7-C), 125.59 (19-C), 126.80 (18-C), 127.82 (7a-C), 128.18 (6-C), 129.30 (5-C), 141.16 (3a-C), 148.34 (16a-C), 149.55 (HC=CHHet), 152.47 (20a-C), 171.96 (2-C) ppm; UV–vis (MeCN) λ_{max} (ε) = 425 nm (27700 M^{-1} cm^{-1}). Anal. calcd for C$_{30}$H$_{42}$Cl$_2$N$_2$O$_{14}$S·1.5H$_2$O (784.65): C, 45.92; H, 5.78; N, 3.57. Found: C, 45.87; H, 5.43; N 3.60%.

3-(6-Ammoniohexyl)-2-[(E)-2-(16-methyl-2,3,5,6,8,9,11,12,15,16-decahydro-14H-1,4,7,10,13,16-benzopentaoxazacyclooctadecin-19-yl)vinyl]-1,3-benzothiazol-3-ium diperchlorate [(E)-**2a**]. A mixture of compound **3a** (57 mg, 0.127 mmol), *N*-methyl(5'-formylbenzo)aza-18-crown-6 ether (50 mg, 0.142 mmol), pyridine (20 µL), and abs. EtOH (5 mL) was heated at 80 °C for 13 h. After cooling to room temperature, the reaction mixture was diluted with benzene (3 mL) and kept for 3 days at –18 °C. The precipitate thus formed was collected on a filter, washed with benzene (3 × 5 mL), and dried in air to give dye (E)-**2a** (65 mg, 65% yield) as red-orange fine-grained crystals, mp 169–170 °C dec; ^{1}H NMR (500.13 MHz, DMSO-d_6, 20 °C) δ 1.34 (m, 2H, CH_2CH$_2$CH$_2$NH$_3$), 1.41 (m, 2H, CH_2CH$_2$CH$_2$N), 1.47 (m, 2H, CH_2CH$_2$NH$_3$), 1.82 (m, 2H, CH_2CH$_2$N), 2.72 (m, 2H, CH_2NH$_3$), 3.03 (s, 3H, Me), 3.51–3.57 (m, 8H, 4 CH$_2$O), 3.57–3.65 (m, 6H, CH_2NMe, 2 CH$_2$O), 3.75 (t, ^3J = 5.9 Hz, 2H, CH_2CH$_2$NMe), 3.85 (m, 2H, CH_2CH$_2$OAr), 4.21 (m, 2H, CH_2OAr), 4.87 (t, ^3J = 7.0 Hz, 2H, CH$_2$N), 6.88 (d, ^3J = 8.4 Hz, 1H, 17-H), 7.53 (d, ^4J = 1.8 Hz, 1H, 20-H), 7.56 (br s, 3H, NH$_3$), 7.60 (dd, ^3J = 8.4 Hz, ^4J = 1.8 Hz, 1H, 18-H), 7.68 (d, ^3J = 15.5 Hz, 1H, HC=CHHet), 7.73 (m, 1H, 6-H), 7.82 (m, 1H, 5-H), 8.11 (d, ^3J = 15.5 Hz, 1H, HC=CHHet), 8.18 (d, ^3J = 8.6 Hz, 1H, 4-H), 8.36 (d, ^3J = 8.6 Hz, 1H, 7-H) ppm; ^{13}C NMR (125.76 MHz, 27 °C) δ 25.15 and 25.31 (CH$_2$$CH_2CH_2CH_2$N), 26.70 ($CH_2CH_2NH_3$), 28.27 ($CH_2CH_2$N), 38.67 (CH$_2NH_3$), 40.82 (Me), 48.00 (CH$_2$N), 53.92 ($CH_2$NMe), 67.78 ($CH_2$OAr), 68.78 ($CH_2CH_2$OAr), 69.17 (CH$_2$O), 69.69 ($CH_2CH_2NMe, CH_2$O), 69.79 (CH$_2$O), 69.93 (CH$_2$O), 70.13 (CH$_2$O), 70.48 (CH$_2$O), 107.73 (HC=$C$HHet), 112.77 (20-C), 115.75 (17-C), 116.09 (4-C), 124.01 (7-C), 124.63 (19-C), 126.64 (18-C), 127.34 (7a-C), 127.70 (6-C), 129.06 (5-C), 141.13 (3a-C), 146.01 (16a-C), 148.74 (20a-C), 149.91(HC=CHHet), 171.27 (2-C) ppm; UV–vis (MeCN) λ_{max} (ε) = 524 nm (35700 M^{-1} cm^{-1}). Anal. calcd for $C_{32}H_{47}Cl_2N_3O_{13}S$ (784.70): C, 48.98; H, 6.04; N 5.36. Found: C, 48.69; H, 6.05; N, 5.44%.

^{1}H NMR titration. MeCN-d_3 (water content < 0.05%, v/v) was used as the solvent. The effective dimerization constants K_D^{eff} for ammonium dyes (E)-**1b,c** and (E)-**2a** were estimated by analyzing the changes in the chemical shifts of some protons ($\Delta\delta_H$) induced by an incremental addition of EtNH$_3$ClO$_4$, as described previously for ammonium dye (E)-**1a**.[8] In these experiments, the dye concentration C_L value was constant (~ (2.5–5)×10^{-3} M) and the total concentration of EtNH$_3$ClO$_4$ (C_S) varied from 0 to ~ 0.14–0.25 M. The $\Delta\delta_H$ values were measured to an accuracy of 0.001 ppm. The experimental dependences of $\Delta\delta_H$ on C_S for different protons were globally fitted to the complexation model represented by equations (1) and (2):

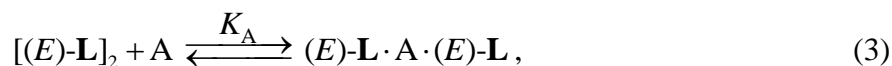$$(E)\text{-}\mathbf{L} + \text{EtNH}_3^+ \xrightleftharpoons{K_S} (E)\text{-}\mathbf{L}\cdot\text{EtNH}_3^+, \tag{1}$$

$$(E)\text{-}\mathbf{L} + (E)\text{-}\mathbf{L} \xrightleftharpoons{K_D} [(E)\text{-}\mathbf{L}]_2, \tag{2}$$

where (E)-$\mathbf{L}$ is the *trans*-isomer of the dye (dication), (E)-$\mathbf{L}\cdot EtNH_3^+$ is the complex of dye and ethylammonium ion, K_S is the stability constant of (E)-$\mathbf{L}\cdot EtNH_3^+$, $[(E)\text{-}\mathbf{L}]_2$ is the dye dimer (tetracation), K_D is the stability constant of dimer $[(E)\text{-}\mathbf{L}]_2$.

These calculations were performed under the assumption that the stability constant K_S (M^{-1}) of the complex formed by the dicationic dye is equal to that for the corresponding model dye having no ammonium group. The calculations did not take into account the activity coefficients of the ions. Therefore the calculated values of the constants K_S are effective (K_S^{eff}). The K_S^{eff} values for model dyes (E)-$\mathbf{1e}$ and (E)-$\mathbf{2b}$ were estimated previously[8,9] by direct ^{1}H NMR titration with $EtNH_3ClO_4$ and then used as fixed parameters in the calculations of K_D^{eff} for (E)-$\mathbf{1b,c}$ and (E)-$\mathbf{2a}$. The equilibrium constants were calculated using the HYPNMR program.[10]

UV-vis spectroscopy. All manipulations with solutions of dyes $\mathbf{1a\text{-}e}$ and $\mathbf{2a,b}$ were performed in a darkroom under red light. The quantitative data on dimerization of dye (E)-$\mathbf{2a}$ were obtained by analyzing the results of three experiments: (*a*) absorption spectra of (E)-$\mathbf{2a}$ measured at seven different dye concentrations ($C_L = 2\times10^{-6}$–3×10^{-4} M; 4.75, 1-, 0.2-, and 0.1-cm cells); (*b*) absorption spectra of the (E)-$\mathbf{2a}$–Bu_4NClO_4 system measured at a constant dye concentration ($C_L = 4\times10^{-6}$ M, 4.75-cm cell) and various concentrations of Bu_4NClO_4 ($SE = 1.8\times10^{-4}$–1.1×10^{-2} M); (*c*) absorption spectra of the (E)-$\mathbf{2a}$–Bu_4NClO_4 system measured at various dye concentrations (2×10^{-6}–3×10^{-4} M; 4.75-, 1-, 0.2-, and 0.1-cm cells) and a constant Bu_4NClO_4 concentration (0.01 M). Only two experiments (*a* and *b*) were carried out for dyes (E)-$\mathbf{1a\text{-}c}$, as the variation of the spectra in experiment (*c*) was moderate. The data from all experiments for each dye were combined, and the resulting matrix of experimental spectra was used to calculate dimerization constant K_D, association constant K_A, and the spectra of the monomer, dimer, and associate using the parameterized matrix modeling (PMM)[11] procedure. The complex formation model included two equilibria (2) and (3).

$$[(E)\text{-}\mathbf{L}]_2 + A \xrightleftharpoons{K_A} (E)\text{-}\mathbf{L}\cdot A\cdot(E)\text{-}\mathbf{L}, \tag{3}$$

where A is the anion (ClO_4^-), (E)-$\mathbf{L}\cdot A\cdot(E)$-$\mathbf{L}$ is the triply charged associate of the dimer with the anion, and K_A is the stability constant of associate (E)-$\mathbf{L}\cdot A\cdot(E)$-$\mathbf{L}$. The procedure used for global analysis of spectral data is described in the Chapter VII.

Photochemistry of free dyes. Solutions were irradiated with a DRSh-250 high-pressure mercury lamp (250 W). The separate spectral lines (313, 365, 405, 436, and 546 nm) were isolated by glass filters. The intensity of light with $\lambda = 546$ nm was measured using a ferrioxalate actinometer. The light intensity at $\lambda = 365$ and 436 nm was determined using a more convenient

system: magnesium complex of 15-crown-5 ether styryl dye (analogue of model dye **1e**), for which the quantum yields of the forward and reverse E–Z-photoisomerizations are known ($\varphi_{E–Z}$ = 0.48 and $\varphi_{Z–E}$ =0.50). Luminescence spectra of dye (E)-**2a** were recorded on an Elumin spectrometer coupled with a PC. The spectra were corrected to take into account the spectral sensitivity of the FEU-79 detector. The fluorescence quantum yields (φ_f) were determined from the corrected spectra using the [Ru(bpy)$_3$]Cl$_2$ complex in water as the reference (φ_f = 0.028). The following relation was used to calculate φ_f:

$$\varphi_f = \varphi_{f\,r}\frac{D_r\,n^2 A}{D\,n_r^{\,2} A_r},$$

where the values with subscript r correspond to the reference compound, D is the solution optical density at the excitation wavelength, n is the refractive index of the solvent, and A is the integral intensity of the corrected fluorescence spectrum in the cm^{-1} scale.

Measurement of the stability constants for the complexes of E-isomers. The stability constants and the absorption spectra of the dye complexes with metal cations were determined by the spectrophotometric titration (SPT) method. The solution ionic strength was maintained at 0.01 M using Bu$_4$NClO$_4$ as the supporting electrolyte. The SPT procedure included recording of the absorption spectra of the dye–metal salt system in MeCN in 1-cm or 4.75-cm cells at various metal ion concentrations and a constant dye concentration. The stability constants of the complexes were determined from the SPT data by the PMM method on the basis of the reaction model including equilibria (2) and (4) for dyes **1a** and **2a** and only equilibrium (4) for model dyes **1e** and **2b**:

$$(E)\text{-}\mathbf{L} + \mathbf{M} \xrightleftharpoons{\;\;K_E\;\;} (E)\text{-}\mathbf{L}\cdot\mathbf{M}\;, \tag{4}$$

where M is the metal ion, K_E is the stability constant of (E)-**L**·M. The measured constants were effective values (K_E^{eff}), since the activity coefficients were not taken into account in the calculations. The known K_D^{eff} values and the absorption spectra of the monomer and dimer of the dye obtained while studying the dye dimerization were used in the calculations. The PMM procedure was similar to that used to calculate K_A and K_D (see Chapter VII).

The stability constants of the complexes (E)-**1a,e**·Ba^{2+} and (E)-**2b**·Ba^{2+} in MeCN were found by competitive SPT. Absorption spectra were measured for solutions of the dye–Ba(ClO$_4$)$_2$–NaClO$_4$ ternary system in a 1-cm cell at various Ba(ClO$_4$)$_2$ concentrations (0–3.3×10^{-4} M range) and a constant dye (C_L ~ 2×10^{-5} M) and NaClO$_4$ (0.01 M) concentrations. The large excess of NaClO$_4$ over the dye and Ba(ClO$_4$)$_2$ ensured minor variation of the solution ionic strength (0.01 M). The SPT data were processed using only equilibrium (4); this gave the observed stability constant K_{obs}. In the ternary systems, there were two equilibria:

$$\mathbf{L} + \mathrm{Na}^+ \; \xrightleftharpoons{K_{\mathrm{Na}}} \; \mathbf{L}\cdot\mathrm{Na}^+ , \tag{5}$$

$$\mathbf{L} + \mathrm{Ba}^{2+} \; \xrightleftharpoons{K_{\mathrm{Ba}}} \; \mathbf{L}\cdot\mathrm{Ba}^{2+} , \tag{6}$$

where $\mathbf{L}$ is the E-isomer of the dye; $\mathbf{L}\cdot\mathrm{Na}^+$ is the sodium complex of the E-isomer of the dye; K_{Na} is the effective stability constant of $\mathbf{L}\cdot\mathrm{Na}^+$; $\mathbf{L}\cdot\mathrm{Ba}^{2+}$ is the barium complex of the E-isomer of the dye; and K_{Ba} is the effective stability constant (K_E^{eff}) of $\mathbf{L}\cdot\mathrm{Ba}^{2+}$. According to the law of mass action, $[\mathbf{L}\cdot\mathrm{Na}^+] = K_{\mathrm{Na}}C_{\mathrm{Na}}[\mathbf{L}]$; here the equilibrium concentration of $[\mathrm{Na}^+]$ is set to be equal to the total concentration C_{Na} due to the large excess of $\mathrm{NaClO_4}$. Then the observed stability constant K_{obs}, measured in competitive SPT, can be written as

$$K_{\mathrm{obs}} = \frac{[\mathbf{L}\cdot\mathrm{Ba}^{2+}]}{[\mathrm{Ba}^{2+}]K_{\mathrm{Na}}C_{\mathrm{Na}}[\mathbf{L}]} , \qquad K_{\mathrm{obs}}K_{\mathrm{Na}}C_{\mathrm{Na}} = \frac{[\mathbf{L}\cdot\mathrm{Ba}^{2+}]}{[\mathrm{Ba}^{2+}][\mathbf{L}]} .$$

Hence, the desired stability constant of the barium complex was found by the equation $K_{\mathrm{Ba}} = K_{\mathrm{obs}}{\times}K_{\mathrm{Na}}{\times}C_{\mathrm{Na}}$.

   Measurement of the stability constants of the complexes of Z-isomers. The target stability constants were also found by the SPT method. In the case of dyes **1a-c**, the SPT procedure was as follows. First a dilute solution of the dye (10 mL) in MeCN ($C_{\mathbf{L}} \sim 4{\times}10^{-6}$ M) containing 0.01 M of $\mathrm{Bu_4NClO_4}$ was irradiated at $\lambda = 436$ nm in a 4.75-cm cell until the photostationary state was attained. The Z-isomer content in this equilibrium state was always > 90%. Then several portions of a MeCN solution containing $\mathrm{Ba(ClO_4)_2}$ in $3.3{\times}10^{-3}$ M concentration were added successively to this solution. The ionic strength of the solution in the cell did not change. At the final stage of SPT, a small portion of the solution containing $\mathrm{Ba(ClO_4)_2}$ in 1 M concentration was added to determine the absorption spectrum of (Z)-dye$\cdot\mathrm{Ba}^{2+}$ more accurately. In the case of **2a**, the photostationary state with a higher content of Z-isomer was formed upon irradiation at $\lambda = 546$ nm. Due to faster dark Z–E-isomerization of dye **2a** compared to benzocrown ether analogues **1a-c**, before the addition of every next portion of the $\mathrm{Ba(ClO_4)_2}$ solution, a new portion of the solution of **2a** was taken and brought to the photostationary state. The resulting spectrophotometric data were processed by PMM method using the reaction model of three equilibria (2), (4), and (7).
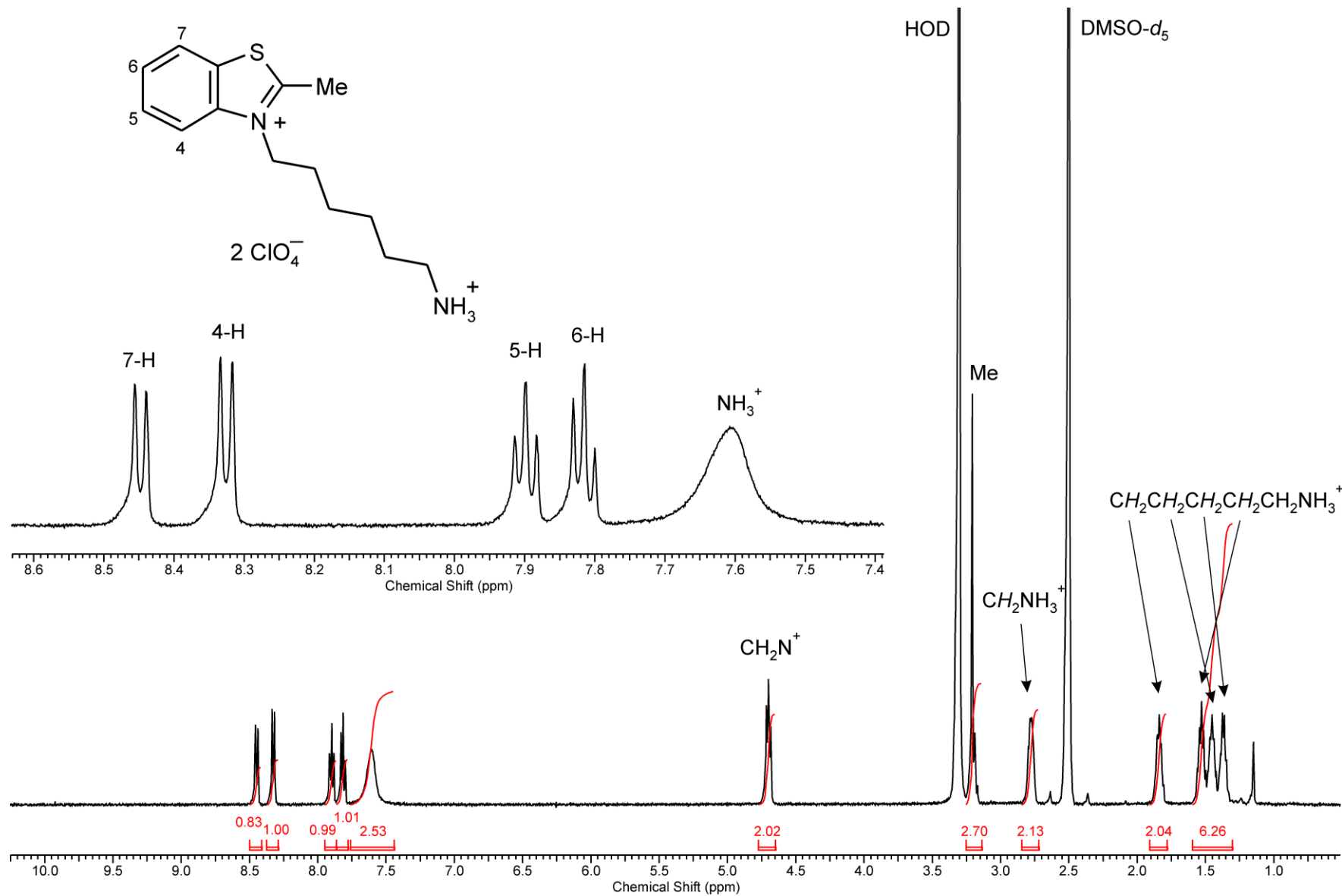
$$(Z)\text{-}\mathbf{L} + \mathrm{M} \; \xrightleftharpoons{K_Z} \; (Z)\text{-}\mathbf{L}\cdot\mathrm{M} , \tag{7}$$

where M is the metal ion (in our case, Ba^{2+}), K_Z is the stability constant of complex (Z)-$\mathbf{L}\cdot$M.
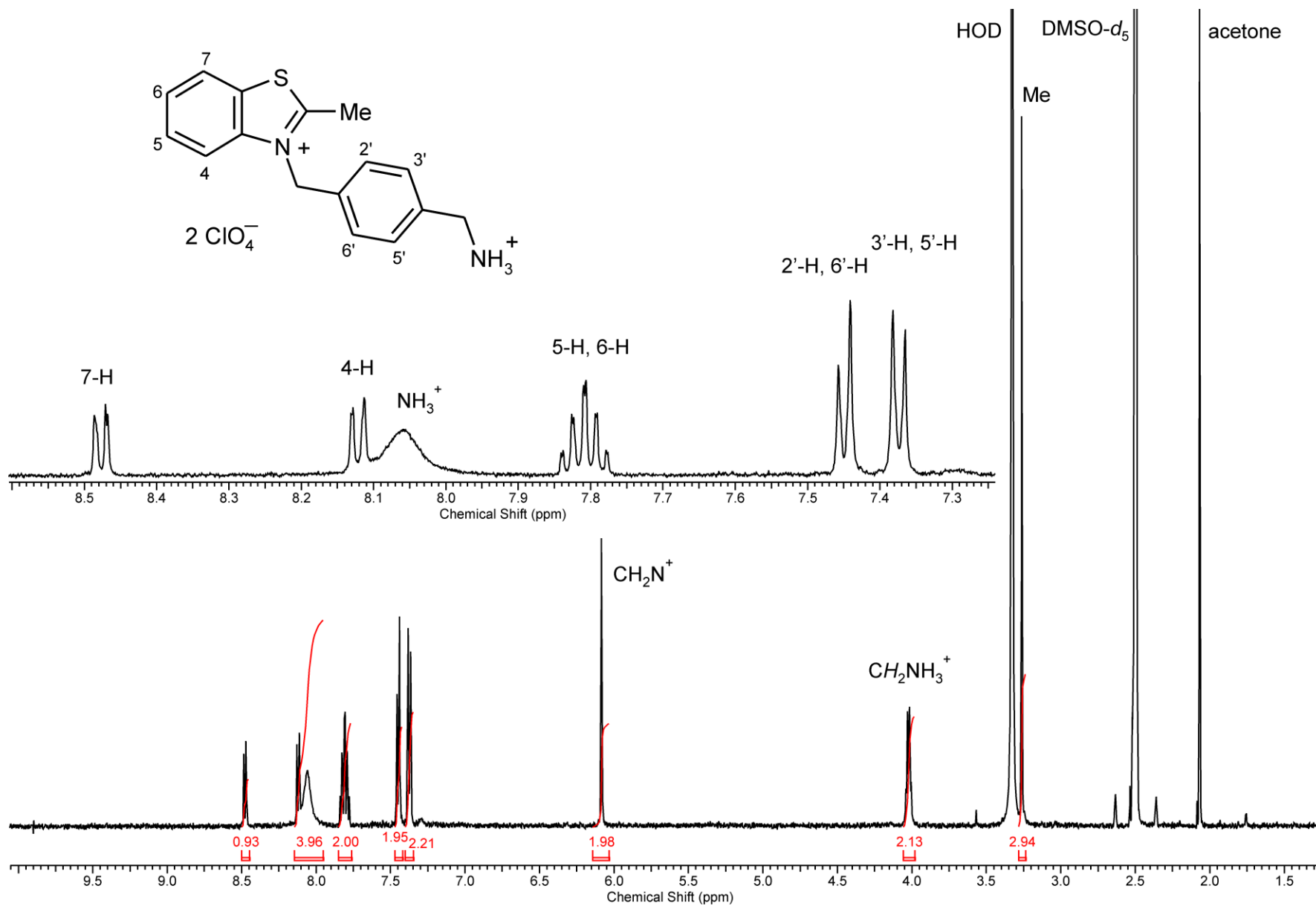
References

1. S. P. Gromov, O. A. Fedorova, A. I. Vedernikov, V. V. Samoshin, N. S. Zefirov and M. V. Alfimov, Synthesis of formyl derivatives of benzocrown ethers containing N, S, and O heteroatoms in the macrocycle, *Russ. Chem. Bull.*, 1995, **44**, 116–123. https://doi.org/10.1007/BF00696971

2. (*a*) S. P. Gromov, S. N. Dmitrieva, A. I. Vedernikov, L. G. Kuz'mina, A. V. Churakov, Yu. A. Strelenko and J. A. K. Howard, Novel promising benzoazacrown ethers as a result of ring transformation of benzocrown ethers: synthesis, structure, and complexation with Ca^{2+}, *Eur. J. Org. Chem.*, 2003, 3189–3199. https://doi.org/10.1002/ejoc.200300179 (*b*) S. P. Gromov, S. N. Dmitrieva, A. I. Vedernikov, N. A. Kurchavov, L. G. Kuz'mina, Yu. A. Strelenko, M. V. Alfimov and J. A. K. Howard, *N*-Methylbenzoazacrown ethers with the nitrogen atom conjugated with the benzene ring: the improved synthesis and the reasons for the high stability of complexes with metal and ammonium cations, *J. Phys. Org. Chem.*, 2009, **22**, 823–833. https://doi.org/10.1002/poc.1527

3. W. G. Bardsley, J. S. Ashford, and C. M. Hill, Synthesis and oxidation of aminoalkyl-onium compounds by pig kidney diamine oxidase, *Biochem. J.*, 1971, **122**, 557–567. https://doi.org/10.1042/bj1220557

4. J. A. Gavin, M. E. Garcia, A. J. Benesi and T. E. Mallouk, Chiral Molecular Recognition in a Tripeptide Benzylviologen Cyclophane Host, *J. Org. Chem.*, 1998, **63**, 7663–7669. https://doi.org/10.1021/jo980352c

5. E. N. Ushakov, A. I. Vedernikov, N. A. Lobova, S. N. Dmitrieva, L. G. Kuz'mina, A. A. Moiseeva, J. A. K. Howard, M. V. Alfimov and S. P. Gromov, Supramolecular dimerization and [2+2] photocycloaddition reactions of crown ether styryl dyes containing a tethered ammonium group: structure–property relationships, *J. Phys. Chem. A*, 2015, **119**, 13025–13037. https://doi.org/10.1021/acs.jpca.5b10758

6. A. I. Vedernikov, D. V. Kondratuk, N. A. Lobova, T. M. Valova, V. A. Barachevskii, M. V. Alfimov and S. P. Gromov, New cation-'capped' complex of the *Z*-isomer of a crown-containing styryl dye bearing a long *N*-ammonioalkyl substituent, *Mendeleev. Commun.*, 2007, **17**, 264–267. https://doi.org/10.1016/j.mencom.2007.09.005

7. S. P. Gromov, S. N. Dmitrieva, A. I. Vedernikov, N. A. Kurchavov, L. G. Kuz'mina, S. K. Sazonov, Yu. A. Strelenko, M. V. Alfimov, J. A. K. Howard and E. N. Ushakov, Synthesis, structure, and characterization of chromo(fluoro)ionophores with cation-triggered emission based on *N*-methylaza-crown-ether styryl dyes, *J. Org. Chem.*, 2013, **78**, 9834–9847. https://doi.org/10.1021/jo401555a

8. A. I. Vedernikov, D. V. Kondratuk, N. A. Lobova, T. M. Valova, V. A. Barachevskii, M. V. Alfimov and S. P. Gromov, New cation-'capped' complex of the *Z*-isomer of a crown-containing styryl dye bearing a long *N*-ammonioalkyl substituent, *Mendeleev. Commun.*, 2007, **17**, 264–267. https://doi.org/10.1016/j.mencom.2007.09.005

9. S. P. Gromov, S. N. Dmitrieva, A. I. Vedernikov, N. A. Kurchavov, L. G. Kuz'mina, S. K. Sazonov, Yu. A. Strelenko, M. V. Alfimov, J. A. K. Howard and E. N. Ushakov, Synthesis, structure, and characterization of chromo(fluoro)ionophores with cation-triggered emission based on *N*-methylaza-crown-ether styryl dyes, *J. Org. Chem.*, 2013, **78**, 9834–9847. https://doi.org/10.1021/jo401555a

10. C. Frassineti, S. Ghelli, P. Gans, A. Sabatini, M. S. Moruzzi and A. Vacca, Nuclear Magnetic Resonance as a Tool for Determining Protonation Constants of Natural Polyprotic Bases in Solution, *Anal. Biochem.*, 1995, **231**, 374–382. https://doi.org/10.1006/abio.1995.9984

11. E. N. Ushakov, S. P. Gromov, O. A. Fedorova, Yu. V. Pershina, M. V. Alfimov, F. Barigilletti, L. Flamigni and V. Balzani, Sandwich-Type Complexes of Alkaline-Earth Metal Cations with a Bisstyryl Dye Containing Two Crown Ether Units, *J. Phys. Chem. A*, 1999, **103**, 11188–11193. https://doi.org/10.1021/jp9929420

Figures S1–S14: ^{1}H and ^{13}C NMR spectra of compounds **1-3**

Figure S1. ^{1}H NMR spectrum of compound **3a** (500.13 MHz, DMSO-d_6, 25 °C).

Figure S2. ^{1}H NMR spectrum of compound **3b** (500.13 MHz, DMSO-d_6, 30 °C).

Figure S3. ^{1}H NMR spectrum of compound **3c** (500.13 MHz, DMSO-d_6, 30 °C).

Figure S4. ^{1}H NMR spectrum of dye (*E*)-**1a** (500.13 MHz, DMSO-d_6, 25 °C).

Figure S5. ^{1}H NMR spectrum of dye (*E*)-**1b** (500.13 MHz, DMSO-d_6, 24 °C).

Figure S6. ^{1}H NMR spectrum of dye (*E*)-**1c** (500.13 MHz, DMSO-*d*$_6$, 30 °C).

Figure S7. ^{1}H NMR spectrum of dye (*E*)-**2a** (500.13 MHz, DMSO-d_6, 20 °C).

Figure S8. ^{13}C NMR spectrum of compound **3a** (125.76 MHz, DMSO-d_6, 24 °C).

Figure S9. ^{13}C NMR spectrum of compound **3b** (125.76 MHz, DMSO-d_6, 24 °C).

Figure S10. ^{13}C NMR spectrum of compound **3c** (125.76 MHz, DMSO-d_6, 24 °C).

Figure S11. ^{13}C NMR spectrum of dye (*E*)-**1a** (125.76 MHz, DMSO-d_6, 30 °C).

Figure S12. ^{13}C NMR spectrum of dye (*E*)-**1b** (125.76 MHz, DMSO-d_6, 25 °C).

Figure S13. ^{13}C NMR spectrum of dye (*E*)-**1c** (125.76 MHz, DMSO-d_6, 30 °C).

Figure S14. ^{13}C NMR spectrum of dye (*E*)-**2a** (125.76 MHz, DMSO-d_6, 27 °C).

III   **Figures S15–S20:** ^{1}H NMR spectra of styryl dyes **1** and **2** with ammonium group, model dyes and their complexes with ethylammoium ion

Figure S15. ^{1}H NMR spectra (aliphatic proton region) of dye (*E*)-**2b** (*a*), mixture of (*E*)-**2b** and EtNH$_3$ClO$_4$ (1:3) (*b*), dye (*E*)-**2a** (*c*), and mixture of (*E*)-**2a** and EtNH$_3$ClO$_4$ (1:49) (*d*) (C_{2b} = 5×10^{-3} M, C_{2a} = 3×10^{-3} M) in MeCN-d_3, 25 °C.

Figure S16. NOESY spectrum of dye (*E*)-**2a** ($C = 2\times10^{-3}$ M) in MeCN-d_3, 23 °C.

Figure S17. ^{1}H NMR spectra (aromatic proton region) of dye (*E*)-**1e** (*a*), mixture of (*E*)-**1e** and EtNH$_3$ClO$_4$ (1:2.8) (*b*), dye (*E*)-**1b** (*c*), and mixture of (*E*)-**1b** and EtNH$_3$ClO$_4$ (1:57) (*d*) ($C_{1e} = 5 \times 10^{-3}$ M, $C_{1b} = 2.6 \times 10^{-3}$ M) in MeCN-d_3, 25 °C.

Figure S18. ^{1}H NMR spectra (aliphatic proton region) of dye (*E*)-**1e** (*a*), mixture of (*E*)-**1e** and EtNH$_3$ClO$_4$ (1:2.8) (*b*), dye (*E*)-**1b** (*c*), and mixture of (*E*)-**1b** and EtNH$_3$ClO$_4$ (1:57) (*d*) ($C_{1e} = 5 \times 10^{-3}$ M, $C_{1b} = 2.6 \times 10^{-3}$ M) in MeCN-d_3, 25 °C.

Figure S19. ^{1}H NMR spectra (aromatic proton region) of dye (*E*)-**1e** (*a*), mixture of (*E*)-**1e** and EtNH$_3$ClO$_4$ (1:2.8) (*b*), dye (*E*)-**1c** (*c*), and mixture of (*E*)-**1c** and EtNH$_3$ClO$_4$ (1:52) (*d*) ($C_{1e} = 5 \times 10^{-3}$ M, $C_{1c} = 5 \times 10^{-3}$ M) in MeCN-d_3, 25 °C.

Figure S20. ^{1}H NMR spectra (aliphatic proton region) of dye (*E*)-**1e** (*a*), mixture of (*E*)-**1e** and EtNH$_3$ClO$_4$ (1:2.8) (*b*), dye (*E*)-**1c** (*c*), and mixture of (*E*)-**1c** and EtNH$_3$ClO$_4$ (1:52) (*d*) (C_{1e} = 5×10^{-3} M, C_{1c} = 5×10^{-3} M) in MeCN-d_3, 25 °C.

Table S1 Effective dimerization equilibrium constants (K_D^{eff}/M^{-1}) for ammonium dyes (E)-**1a-d** and effective stability constants (K_S^{eff}/M^{-1}) for the 1:1 complexes of model dyes (E)-**1e** and (E)-**2b** with EtNH$_3^+$ derived from ^{1}H NMR titration with EtNH$_3$ClO$_4$.[a]

Dye	logK_D^{eff}	Dye	logK_S^{eff}
(E)-**1a**	6.1 [b]	(E)-**1e**	3.5 [b]
(E)-**1b**	5.6		
(E)-**1c**	6.3		
(E)-**1d**	5.9 [c]		
(E)-**2a**	4.3	(E)-**2b**	3.0 [d]

[a] MeCN-d_3, 25±1 °C, the equilibrium constants were measured to within ~30%. [b] Ref 22 (in article). [c] Ref 34 (in article). [d] Ref 35 (in article).
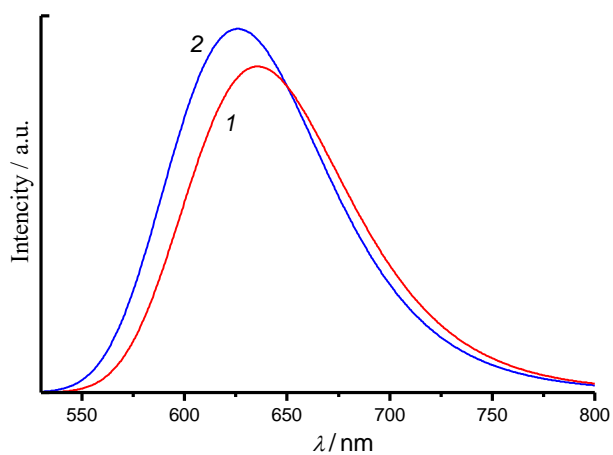
V   **Figures S21–S24:** Absorption and luminescence spectra of free dyes **1**, **2**
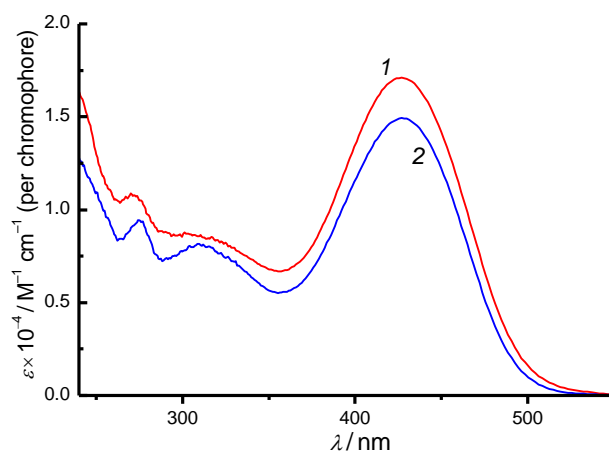

Fig. S21. Absorption spectra of dye **1e** in MeCN: (*1*) *E*-isomer; (*2,3*) photosationary states (PSS) obtained by irradiation at 365 and 436 nm, respectively; (*4*) calculated by the Fisher method using the PMM spectrum of the *Z*-isomer.

Fig. S22. Absorption spectra of the dyes in MeCN: *a)* **1a**; *b)* **1b**; *c)* **1c**; *d)* **2a**; (curves *1,2*) monomeric and dimeric forms of the *E*-isomer; (black curve *3*) intramolecular complex of the *Z*-isomer.
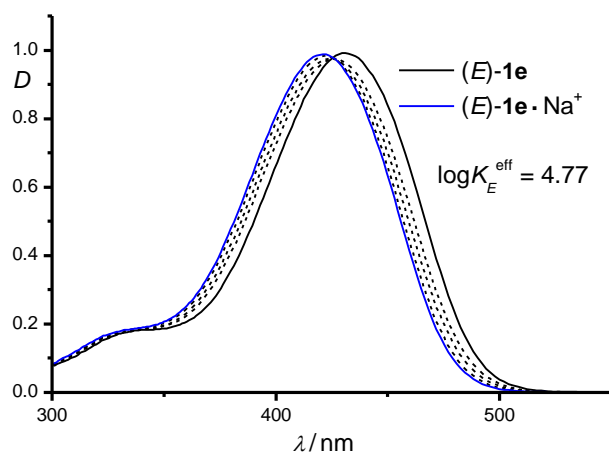
Fig. S23. Corrected luminescence spectra of monomeric (*1*) and dimeric (*2*) forms of (*E*)-**2a** in MeCN; the spectra are normalized in such a way that the ratio of the integral intensities on the energy scale corresponds to the ratio of the luminescence quantum yields.
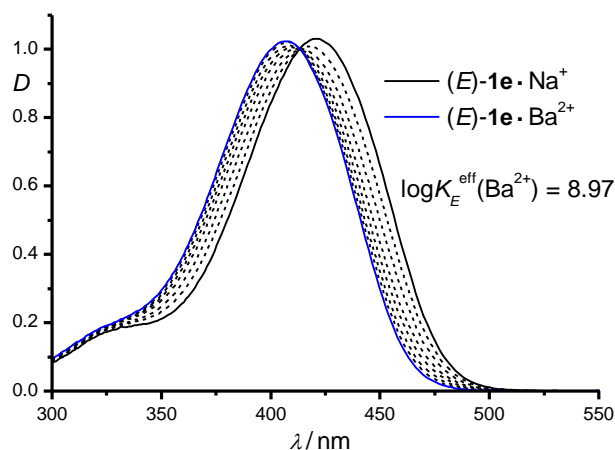

Fig. S24. Absorption spectra of the photostationary states achieved by irradiation of dyes **1d** (*1*) and **1e** (*2*) with 436 nm light in MeCN.
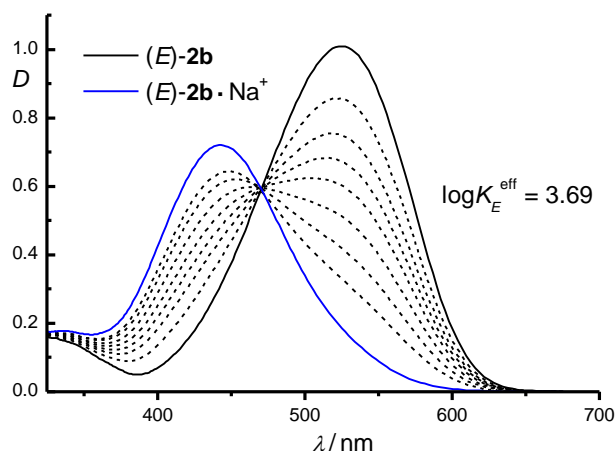
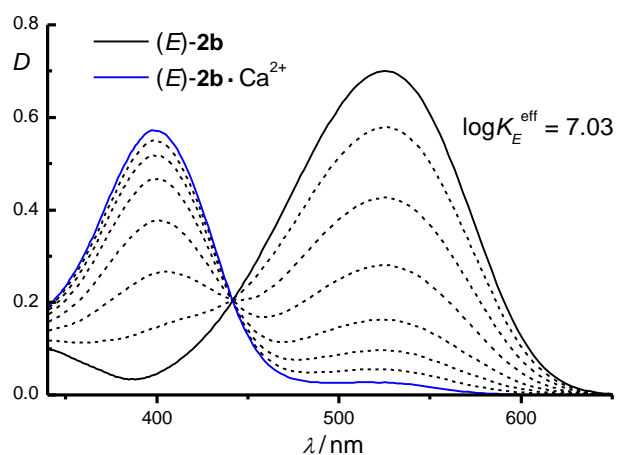VI   **Figures S25–S36:** Spectrophotometric titration data

Fig. S25. Absorption spectra of the (*E*)-**1e**–NaClO$_4$ system in MeCN: $l = 1$ cm, the concentration of the ligand (*E*)-**1e** is constant (2.6×10^{-5} M), the concentration of NaClO$_4$ is varied from 0 to 1.3×10^{-3} M, the ionic strength I is kept constant at 0.01 M using Bu$_4$NClO$_4$ as a supporting electrolyte.
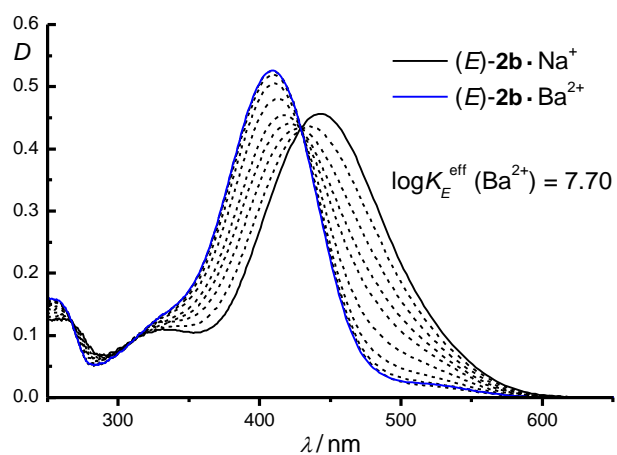

Fig. S26. Absorption spectra of the (*E*)-**1e**–Na(ClO$_4$)$_2$–Ba(ClO$_4$)$_2$ system in MeCN: $l = 1$ cm, the concentrations of the ligand (*E*)-**1e** and NaClO$_4$ are constant (2.7×10^{-5} M and 0.01 M, respectively), the concentration of Ba(ClO$_4$)$_2$ is varied from 0 to 3.3×10^{-4} M.
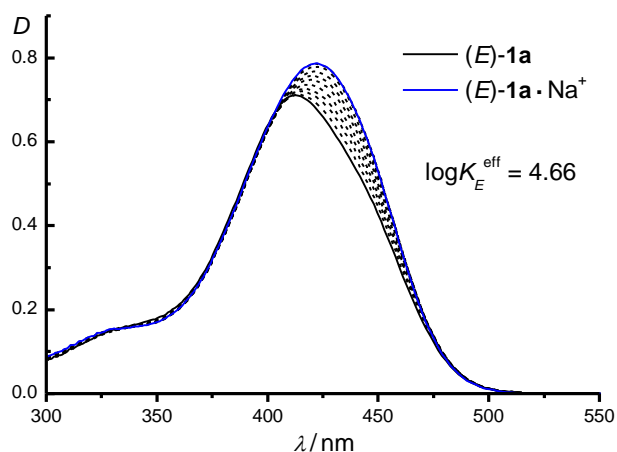

Fig. S27. Absorption spectra of the (*E*)-**2b**–NaClO$_4$ system in MeCN: $l = 1$ cm, the concentration of the ligand (*E*)-**2b** is constant (2.3×10^{-5} M), the concentration of NaClO$_4$ is varied from 0 to 9.0×10^{-4} M, the ionic strength I is kept constant at 0.01 M using Bu$_4$NClO$_4$ as a supporting electrolyte.
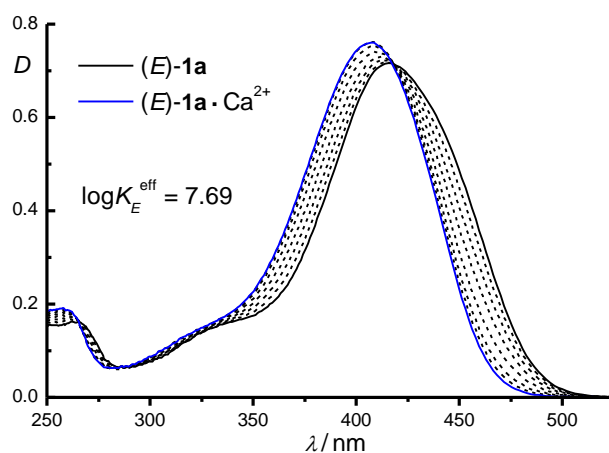
Fig. S28. Absorption spectra of the (*E*)-**2b**–Ca(ClO$_4$)$_2$ system in MeCN: *l* = 4.75 cm, the concentration of the ligand (*E*)-**2b** is constant (3.4×10^{-6} M), the concentration of Ca(ClO$_4$)$_2$ is varied from 0 to 1.3×10^{-5} M, the ionic strength *I* is kept constant at 0.01 M using Bu$_4$NClO$_4$ as a supporting electrolyte.

Fig. S29. Absorption spectra of the (*E*)-**2b**–Na(ClO$_4$)$_2$–Ba(ClO$_4$)$_2$ system in MeCN: *l* = 1 cm, the concentrations of the ligand (*E*)-**2b** and NaClO$_4$ are constant (1.5×10^{-5} M and 0.01 M, respectively), the concentration of Ba(ClO$_4$)$_2$ is varied from 0 to 2.4×10^{-4} M.

Fig. S30. Absorption spectra of the (*E*)-**1a**–NaClO$_4$ system in MeCN: *l* = 1 cm, the concentration of the ligand (*E*)-**1a** is constant (2.1×10^{-5} M), the concentration of NaClO$_4$ is varied from 0 to 1.7×10^{-2} M, the ionic strength *I* is kept constant at 0.01 M using Bu$_4$NClO$_4$ as a supporting electrolyte.

Fig. S31. Absorption spectra of the (*E*)-**1a**–Ca(ClO$_4$)$_2$ system in MeCN: l = 4.75 cm, the concentration of the ligand (*E*)-**1a** is constant (4.6×10^{-6} M), the concentration of Ca(ClO$_4$)$_2$ is varied from 0 to 2.8×10^{-5} M, the ionic strength I is kept constant at 0.01 M using Bu$_4$NClO$_4$ as a supporting electrolyte.
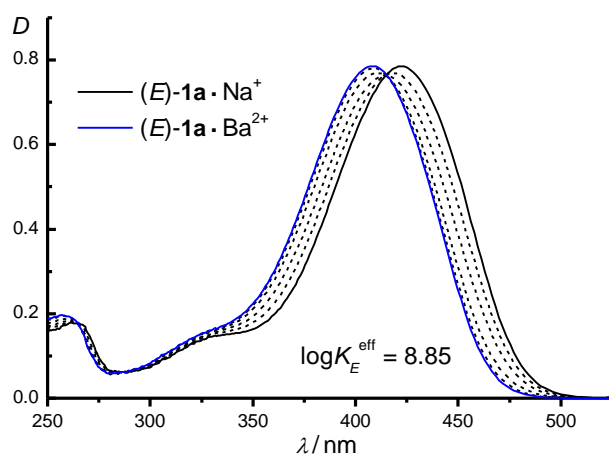

Fig. S32. Absorption spectra of the (*E*)-**1a**–Na(ClO$_4$)$_2$–Ba(ClO$_4$)$_2$ system in MeCN: l = 1 cm, the concentrations of the ligand (*E*)-**1a** and NaClO$_4$ are constant (2.1×10^{-5} M and 0.01 M, respectively), concentration of Ba(ClO$_4$)$_2$ is varied from 0 to 3.3×10^{-4} M.
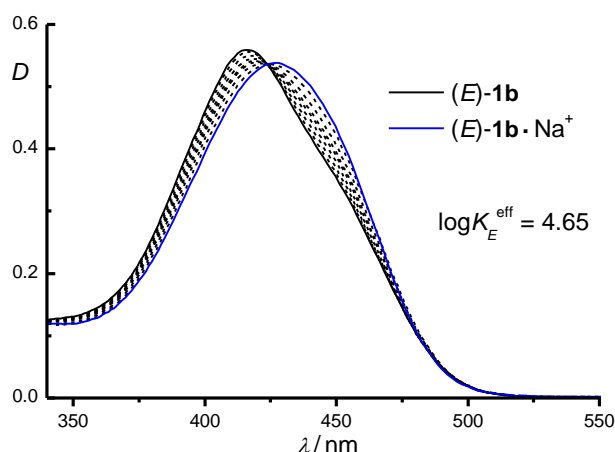

Fig. S33. Absorption spectra of the (*E*)-**1b**–NaClO$_4$ system in MeCN: l = 1 cm, the concentration of the ligand (*E*)-**1b** is constant (1.6×10^{-5} M), the concentration of NaClO$_4$ is varied from 0 to 4.9×10^{-4} M, the ionic strength I is kept constant at 0.01 M using Bu$_4$NClO$_4$ as a supporting electrolyte.
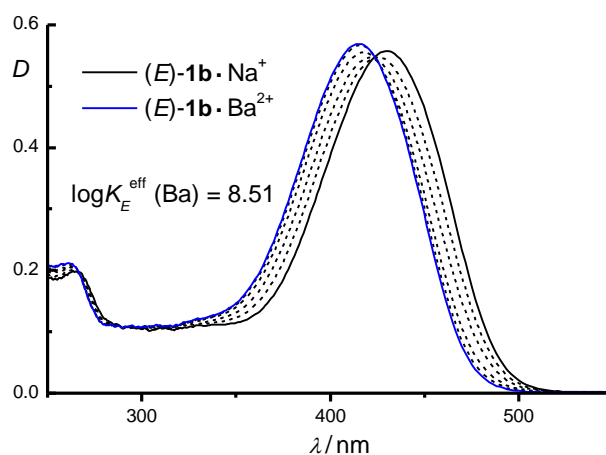
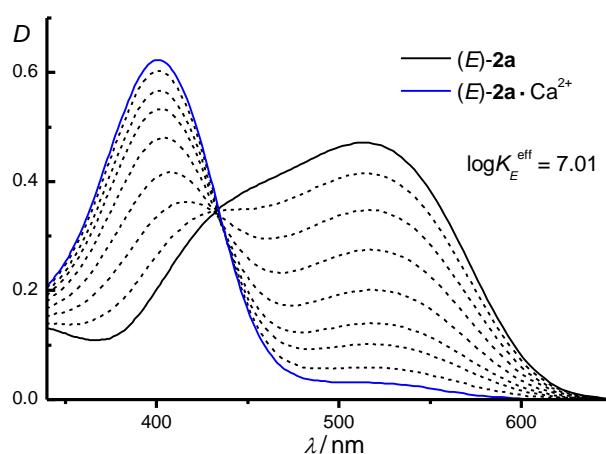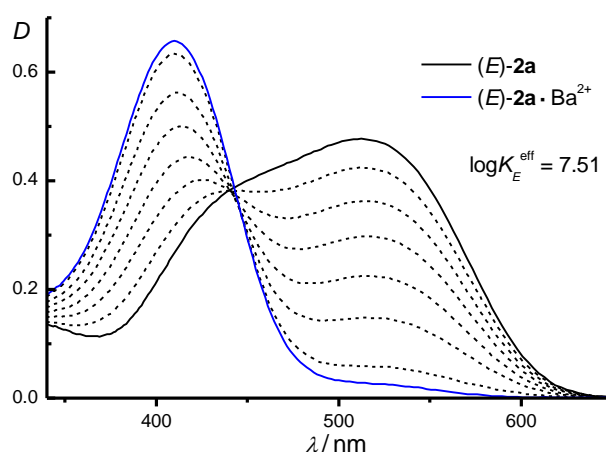**Fig. S34.** Absorption spectra of the (*E*)-**1b**–Na(ClO$_4$)$_2$–Ba(ClO$_4$)$_2$ system in MeCN: l = 1 cm, the concentrations of the ligand (*E*)-**1b** and NaClO$_4$ are constant (1.6×10^{-5} M and 0.01 M, respectively), the concentration of Ba(ClO$_4$)$_2$ is varied from 0 to 1.3×10^{-4} M.

Fig. S35. Absorption spectra of the (*E*)-**2a**–Ca(ClO$_4$)$_2$ system in MeCN: l = 4.75 cm, the concentration of the ligand (*E*)-**2a** is constant (3.7×10^{-6} M), the concentration of Ca(ClO$_4$)$_2$ is varied from 0 to 1.4×10^{-5} M, the ionic strength I is kept constant at 0.01 M using Bu$_4$NClO$_4$ as a supporting electrolyte.

Fig. S36. Absorption spectra of the (*E*)-**2a**–Ba(ClO$_4$)$_2$ system in MeCN: l = 4.75 cm, the concentration of the ligand (*E*)-**2a** is constant (3.8×10^{-6} M), the concentration of Ba(ClO$_4$)$_2$ is varied from 0 to 1.3×10^{-5} M, the ionic strength I is kept constant at 0.01 M using Bu$_4$NClO$_4$ as a supporting electrolyte.

VII   Parameterized matrix modeling of spectral data of the dimerization

The number of light-absorbing species in the systems was estimated by the abstract factor analysis of the absorption spectra obtained in various experiments. These spectra were used to compose the data matrix $\mathbf{D}_{exp}$ with dimensions $n \times m$ (n is the number of optical density values in the spectrum, m is the number of spectra). The matrix was then subjected to a singular vector and singular value decomposition. The singular decomposition was performed in the Matlab7 program using the "svd" function. Singular vectors have a remarkable feature: if there are k light-absorbing components in the system, the absorption spectra of this system measured at various component concentrations can be represented as a linear combination of the first k vectors of the singular decomposition of the data matrix $\mathbf{D}_{exp}$ (the other vectors describe the instrumental errors of spectral measurements). Exceptions are systems in which the concentrations of separate components vary in proportion to one another or in which the spectrum of a particular component can be represented as a linear combination of the spectra of other components. In these cases, the number of significant vectors of singular decomposition is less than the number of components.

The calculations showed that for each of the systems, the experimental spectra (i.e., the matrix $\mathbf{D}_{exp}$, Fig. 3) are satisfactorily approximated by two principal singular decomposition vectors (in all cases, the standard deviation for the approximation was < 0.001 in the optical density units).

Attempts to describe the concentration dependences of the absorption spectra of (E)-**1a–c** and (E)-**2a** using the simple dimerization model consisting of only one equilibrium were unsuccessful. Using a heuristic approach, we found that these dependences can be described by the following reaction model:

$$L + L \; \underset{\longleftarrow}{\overset{K_D}{\longrightarrow}} \; LL , \qquad (1)$$

$$LL + A \; \underset{\longleftarrow}{\overset{K_A}{\longrightarrow}} \; L \cdot A \cdot L , \qquad (2)$$

where L is the E-isomer of the dye (dication), LL is the dimer of the E-isomer (tetracation), A is the anion (ClO_4^-), and LAL is the triply charged associate of the dimer with the anion.

The mass balance equations for this model are as follows:

$$2[LAL] + 2[LL] + [L] = C_L, \qquad (3)$$

$$[LAL] + [A] = 2C_L + SE, \qquad (4)$$

where C_L is the total dye concentration, SE is the total concentration of the supporting electrolyte (Bu_4NClO_4 or $Bu_4NClO_4/HClO_4$).

Law of mass action:

$$[LL] = \frac{\gamma_L^2}{\gamma_{LL}} K_D[L]^2, \tag{5}$$

$$[LAL] = \frac{\gamma_{LL}\gamma_A}{\gamma_{LAL}} K_A[LL][A] \tag{6}$$

where γ_L, γ_{LL}, γ_A, and γ_{LAL} are the activity coefficients of the ions.

We will use the following designations: $x = [LL]/C_L$, $k_1 = \gamma_L^2/\gamma_{LL}$, and $k_2 = (\gamma_{LL}\gamma_A)/\gamma_{LAL}$. The set of equations (3)–(6) can be reduced to the following equation

$$2k_2 K_A C_L x^2 + (3k_2 K_A C_L + 2k_2 K_A SE + 2)x + (k_2 K_A C_L x + 1)\sqrt{\frac{x}{k_1 K_D C_L}} - 1 = 0 \tag{7}$$

The ion activity coefficients are determined using the Debye-Hückel formula:

$$\log \gamma = -\frac{B_1 z^2 \sqrt{IS}}{1 + B_2 d \sqrt{IS}}, \tag{8}$$

where z is the ion charge, d is the conventional ion diameter, IS is the ionic strength, and B_1 and B_2 are the coefficients in the Debye-Hückel formula

$$B_1 = 1.824 \times 10^6 (\varepsilon T)^{-1.5}, \; B_2 = 50.29(\varepsilon T)^{-0.5},$$

where ε is the dielectric constant of the solvent, T is temperature. For acetonitrile ($\varepsilon = 37$), $B_1 = 1.6$, and $B_2 = 0.48$ (for $T = 295$ K). The perchlorate ion diameter d_A was taken to be 3 Å, and the tetracation d_{LL} and associate d_{LAL} diameters were assumed to be 22 Å. The diameter of the dye dication d_L was determined in the parametric modeling of the spectra (see below).

Ionic strength of the solution

$$IS = (z_{LAL}^2[LAL] + z_{LL}^2[LL] + z_L^2[L] + 2C_L - [LAL] + 2SE)/2, \tag{9}$$

where $z_L = 2$, $z_{LL} = 4$, and $z_{LAL} = 3$. Using equation (3), one gets

$$IS = (3 + 3x)C_L + SE. \tag{10}$$

The absorption spectra of the monomeric and dimeric dyes (E)-**1a-c** and (E)-**2a** and the equilibrium constants K_D and K_A were found by parameterized matrix modeling (PMM). The total dye concentrations C_L were determined from the optical density of the solutions at a wavelength at which the molar absorption coefficients of the monomeric and dimeric forms were equal.

The PMM procedure was started from the postulation of K_D, K_A, and d_L and numerical solution of the set of equations (7), (8), and (10) for x. The numerical solution was found using the function "fminbnd" in Matlab7. The monomer concentration [L] was derived from equation (5) and the associate concentration [LAL] was calculated from the mass balance equation (3).

According to the results of abstract factor analysis (see above), the tetracation LL and the associate LAL had identical absorption spectra. Therefore, the total concentration of dimeric

forms of the dye, [D] = [LL] + [LAL], was used in the calculations. The [L] and [D] values found in this way were multiplied by the cell length *l*, and the results were used to compose the concentration matrix **C** with the dimensions *2×m* composed of the [L]*l* and [D]*l* values corresponding to *m* measured absorption spectra. Then the *n×m* matrix **D**$_{exp}$ composed of *m* experimental spectra was used to generate an *n × 2* theoretical matrix of the molar absorption coefficients of the components (**E**$_{cal}$):

$$\mathbf{E}_{cal} = \mathbf{D}_{exp}\mathbf{C}^{T}(\mathbf{C}\mathbf{C}^{T})^{-1}. \tag{11}$$

Equation (11) is nothing but the solution to the matrix representation of the light absorption law **D** = **EC**. The theoretical matrix **D**$_{cal}$, reproducing **D**$_{exp}$, was calculated as **D**$_{cal}$ = **E**$_{cal}$**C**.

The K_D, K_A, and d_L values and the absorption spectra of the monomer and dimer were found by minimizing the standard deviation $\sigma_D(K_D, K_A, d_L)$ between the theoretical matrix **D**$_{cal}$ and the matrix of experimental spectra **D**$_{exp}$:

$$\sigma_D(K_D, K_A, d_L) = \sqrt{\frac{\sum_{i=1}^{n}\sum_{j=1}^{m}(D_{exp}^{ij} - D_{cal}^{ij})^2}{(n-k)m}}. \tag{12}$$

Minimization was performed using the function "fminsearch" in Matlab7. The σ_D value is the criterion for the validity of the reaction model. Apart from the instrumental errors, it contains errors of the measurement of concentrations, cell length, *etc.* Previously, it was established by experiments that $\sigma_D < 0.002$ is adequate for the instruments and techniques that we use.